Research Square

Preprints are preliminary reports that have not undergone peer review.
They should not be considered conclusive, used to inform clinical practice,
or referenced by the media as validated information.

Circ_0072088 regulates EMT-associated and fibrogenic changes through the miR-330-3p/CDK1 axis in AML12 hepatocytes

Yingying Cheng
Harbin Medical University Cancer Hospital
Houshuang Xu
Harbin Medical University Cancer Hospital
Baojun Li
Harbin Medical University Cancer Hospital
Jifu Qin
Heilongjiang Provincial Hospital
Guofu Li
liguofu1012@hrbmu.edu.cn

Harbin Medical University Cancer Hospital

Research Article

Keywords: Hepatic fibrosis, circRNAs, miRNAs, CDK1, epithelial-mesenchymal transition

Posted Date: November 20th, 2026

DOI: https://doi.org/10.21203/rs.3.rs-11786894/v1

License: This work is licensed under a Creative Commons Attribution 4.0 International License.
Read Full License

Additional Declarations: No competing interests reported.

Circ_0072088 regulates EMT-associated and fibrogenic changes through the miR-330-3p/CDK1 axis in AML12 hepatocytes

Yingying Cheng[1], Houshuang Xu[2], Baojun Li[3], Jifu Qin[4], Guofu Li[2,*]

1Department of Ultrasound, Harbin Medical University Cancer Hospital, Harbin, China.

2Department of Neurosurgery, Harbin Medical University Cancer Hospital, Harbin, China

3Department of Head and NJeck Surgery, Harbin Medical University Cancer Hospital, Harbin, China

4Second Department of Gastroenterology, Heilongjiang Provincial Hospital, Harbin, China

Running title: Circ_0072088 facilitated hepatic fibrosis

Abstract

Background: Circular RNAs (circRNAs) have been implicated in liver fibrosis, but the role of circ_0072088 remains unclear. This study investigated the involvement of circ_0072088 in transforming growth factor-β1 (TGF-β1)-induced epithelial–mesenchymal transition (EMT)-associated and fibrogenic changes in AML12 hepatocytes.

Methods and Results: AML12 cells were treated with TGF-β1 and subjected to circ_0072088, miR-330-3p, or CDK1 manipulation. RNA and protein expression were assessed using reverse transcription–quantitative PCR and western blotting, respectively. RNA interaction assays and dual-luciferase reporter assays were used to investigate the proposed regulatory interactions. Cell viability was assessed using the Cell Counting Kit-8 assay. TGF-β1 increased circ_0072088 expression in a time-dependent manner. Circ_0072088 knockdown increased E-cadherin expression and decreased α-smooth muscle actin, vimentin, and collagen I and IV levels. Interaction assays supported an association between circ_0072088 and miR-330-3p,

while reporter assays supported CDK1 as a miR-330-3p target. MiR-330-3p overexpression attenuated the effects of circ_0072088 overexpression, whereas CDK1 overexpression counteracted the effects of miR-330-3p. Inhibition of miR-330-3p also reversed the reduction in CDK1 protein levels induced by circ_0072088 knockdown. **Conclusions:** These findings support a role for the circ_0072088/miR-330-3p/CDK1 axis in regulating EMT-associated and fibrogenic changes in AML12 cells. Further studies are needed to establish its relevance to liver fibrosis in vivo.

Keywords: Hepatic fibrosis; circRNAs; miRNAs; CDK1; epithelial-mesenchymal transition

Abbreviations: HCC, hepatocellular cancer; EMT, epithelial-mesenchymal transition; miRNA, microRNA; ECM, extracellular matrix; circRNAs, circular RNAs; UTR, untranslated region; HSCs, hepatic stellate cells; FBS, fetal bovine serum; NC, negative controls; AMO, anti-miRNA oligonucleotide; DMEM, Dulbecco's Modifified Eagle's Medium; MUT, mutated; WT, wild-type; CCK8, Cell Counting Kit-8; OD, optical density.

Introduction

Hepatic fibrosis is characterized by excessive extracellular matrix (ECM) deposition and disruption of normal liver architecture[1]. Progressive fibrosis can lead to cirrhosis and liver failure and is associated with an increased risk of hepatocellular carcinoma (HCC)[2, 3]. Epithelial–mesenchymal transition (EMT)-associated changes have been investigated in models of hepatic, renal, and pulmonary fibrosis[4–6]. In hepatocyte models, transforming growth factor-β1 (TGF-β1) induces changes in epithelial, mesenchymal, and fibrogenic markers[7, 8]. These cellular changes provide a basis for investigating pathways associated with liver injury, although their contribution to tissue fibrosis requires further validation. Therapeutic options remain limited and depend on the underlying cause and stage of liver disease. A better

understanding of the molecular pathways involved may help identify potential targets for further investigation.

Non-coding RNAs have attracted increasing attention because of their involvement in diverse physiological and pathological processes[9, 10]. Circular RNAs (circRNAs) are characterized by covalently closed RNA structures and can regulate gene expression through interactions with other RNAs[11, 12]. MicroRNAs (miRNAs) regulate gene expression by binding complementary sequences in target mRNAs, frequently within the 3′-untranslated region (3′-UTR)[13]. Some circRNAs interact with miRNAs and may function as molecular sponges, thereby modulating downstream gene expression[14, 15]. Dysregulated circRNA and miRNA expression has been associated with hepatic fibrosis[16, 17]. However, the functions and regulatory partners of individual circRNAs remain incompletely understood.

Circ_0072088 is upregulated in HCC. In human HCC cell lines, including HepG2 and SNU-398, circ_0072088 has been reported to promote proliferation and migration and inhibit apoptosis through the miR-375/JAK2/STAT3 pathway[18]. These findings suggest that circ_0072088 participates in the regulation of hepatocellular phenotypes. However, its role in fibrogenic responses remains unclear.

In this study, we investigated the role of circ_0072088 in TGF-β1-treated AML12 hepatocytes and examined the involvement of the miR-330-3p/CDK1 axis. We combined RNA and protein expression analyses with interaction assays and rescue experiments to assess whether this regulatory axis contributes to EMT-associated and fibrogenic changes in this cellular model.

Materials and Methods

Cell culture

AML12 cells, an immortalized mouse hepatocyte cell line (cat. no. CM3062; Cell Bank of the Chinese Academy of Sciences, Shanghai, China), were maintained in a 1:1 mixture of Dulbecco's modified Eagle's medium (DMEM) and Ham's F-12 medium (cat. no. 11330057; Gibco, USA) supplemented with a premixed insulin–

transferrin–selenium preparation (ITS; 5 μg/mL), 10% fetal bovine serum (FBS; HyClone, GE Healthcare Life Sciences), and 1% penicillin/streptomycin. Cells were cultured at 37 °C in a humidified atmosphere containing 5% CO_2. TGF-β1 (2 ng/mL; R&D Systems, USA) was used to induce EMT-associated and fibrogenic changes.

Cell transfection

Circ_0072088 and CDK1 sequences were cloned into pcDNA3.1 plasmids to generate overexpression constructs. The overexpression constructs were supplied by Aibosi (Shanghai, China). At approximately 70% confluence, AML12 cells were transfected with pcDNA3.1-circ_0072088, pcDNA3.1-CDK1, si-circ_0072088, antimiRNA oligonucleotide (AMO)-330-3p, miR-330-3p mimics, or the corresponding negative controls (NCs), as indicated, using Lipofectamine 2000 (cat. no. 11668019; Invitrogen, USA). After 6 h, the transfection medium was replaced with complete medium, and cells were cultured for a further 48 h at 37 °C.

Reverse transcription–quantitative PCR

Total RNA was extracted from AML12 cells using 1 mL of TRIzol reagent (cat. no. 15596018; Invitrogen, USA). RNA (1 μg) was reverse-transcribed using a reverse transcription kit (cat. nos. QPK212 and FSQ-101; Toyobo, Japan) with random primers. Quantitative PCR was performed using SYBR Green PCR Master Mix (cat. no. QPK212; Toyobo, Japan). MiR-330-3p expression was normalized to U6, and circ_0072088 expression was normalized to GAPDH. Relative expression was calculated using the $2^{-}\Delta\Delta Ct$ method.

The sequences of the primers used in this study are presented in Table I.

Table I:Primer sequences

Name		Primer sequences
Circ_0072088	Forward	AATGGTCTGCAGTCCTGTGT
	Reverse	TGCCTGTAACTCCTCTTCAGT

miR-330-3p	Forward	CGGCAAAGCACACGGCCTG
	Reverse	TGCGTGTCGTGGAGTCGGC
GAPDH	Forward	ACTCCACTCACGGCAAATTC
	Reverse	TCTCCATGGTGGTGAAGACA
U6	Forward	CTCGCTTCGGCAGCACA
	Reverse	AACGCTTCACGAATTTGCGT

Western bloting

Proteins were extracted from AML12 cells on ice using RIPA lysis buffer (cat. no. R0020; Solarbio, China) supplemented with 1% protease inhibitors. Protein concentrations were measured using a BCA assay (cat. no. P0012; Beyotime, China). Samples were separated by 10% SDS-PAGE and transferred to nitrocellulose membranes. The membranes were blocked with 5% non-fat milk in phosphate-buffered saline (PBS) for 2 h and incubated overnight at 4 °C with primary antibodies against α-smooth muscle actin (α-SMA; 1:500; cat. no. 19245; Cell Signaling Technology, USA), E-cadherin (1:1,000; cat. no. 14472; Cell Signaling Technology), vimentin (1:1,000; cat. no. 5741; Cell Signaling Technology), CDK1 (1:5,000; cat. no. ab133327; Abcam, USA), collagen I (1:1,000; cat. no. ab34710; Abcam), collagen IV (1:500; cat. no. ab214417; Abcam), and GAPDH (1:1,000; cat. no. TA-08; Zhongshanjinqiao, China). The membranes were then incubated with a secondary antibody (1:10,000; cat. no. 92632211; LI-COR, USA) for 1 h at room temperature. Bands were visualized using an Odyssey imaging system with version 3.0 software (LI-COR Biosciences, USA). Band intensities were quantified as band area multiplied by optical density.

Dual-luciferase reporter assays

Potential miR-330-3p-binding sites in circ_0072088 and the CDK1 3′-UTR were predicted using CircInteractome and TargetScan, respectively. Sequences containing the predicted wild-type (WT) or mutant (MUT) binding sites were cloned into psiCHECK-2 reporter vectors (Promega, USA). HEK293T cells were co-transfected with the WT or MUT reporter constructs (100 mg) and either miR-330-3p mimics or

mimic NC using Lipofectamine 2000 (cat. no. 11668019; Invitrogen, USA). Luciferase activity was measured using a dual-luciferase reporter assay system (Promega, USA).

RNA Pull-Down Assay

Biotinylated circ_0072088 or miR-330-3p probes were incubated with streptavidin magnetic beads (Thermo Fisher Scientific, USA) for 2 h. The probe-bound beads were subsequently incubated with AML12 cell samples overnight at 4 °C. Associated RNA was analyzed by RT-qPCR to assess the interaction between circ_0072088 and miR-330-3p.

Cell viability assay

Cell viability was assessed using the Cell Counting Kit-8 assay (CCK-8; cat. no. CK04; Dojindo, Japan). At approximately 70% confluence, AML12 cells were seeded in 96-well plates at 1×10^4 cells/well and subjected to the indicated transfections, followed by TGF-β1 treatment for 48 h. CCK-8 working solution was then added at 10%, and the cells were incubated at 37 °C for 1 h. Absorbance was measured at 450 nm.

Statistical analysis

Data are presented as the mean ± standard error of the mean (SEM). Each experiment was performed independently at least five times. Differences among multiple groups were analyzed using one-way analysis of variance (ANOVA). $P < 0.05$ was considered statistically significant. Statistical analyses were performed using GraphPad Prism version 5.0 (GraphPad Software, USA).

Results

TGF-β1 increases circ_0072088 expression in AML12 cells

To investigate the response of circ_0072088 to TGF-β1, its expression was measured by RT-qPCR in AML12 cells treated with or without TGF-β1. Circ_0072088 expression increased in a time-dependent manner following TGF-β1 treatment compared with the control group (Fig. 1A).

Circ_0072088 knockdown attenuates EMT-associated and fibrogenic changes

RT-qPCR confirmed that si-circ_0072088 reduced circ_0072088 expression in AML12 cells (Fig. 1B). Western blotting showed that circ_0072088 knockdown increased E-cadherin levels and decreased α-SMA and vimentin levels (Fig. 1C–F). Collagen I and IV protein levels were also reduced (Fig. 1G–I), indicating lower expression of ECM-associated proteins. In addition, circ_0072088 knockdown increased the CCK-8 signal, consistent with improved cell viability (Fig. 1J). These findings suggest that circ_0072088 knockdown attenuates EMT-associated and fibrogenic changes in this cellular model.

Circ_0072088 interacts with miR-330-3p

CircInteractome analysis identified a potential miR-330-3p-binding site in circ_0072088 (Fig. 2A). MiR-330-3p expression decreased over time in TGF-β1-treated AML12 cells, showing an inverse pattern to circ_0072088 expression (Fig. 2B). Dual-luciferase reporter assays showed that miR-330-3p mimics reduced the activity of the WT circ_0072088 reporter but did not affect the MUT reporter in HEK293T cells (Fig. 2C). RNA interaction assays showed greater enrichment of circ_0072088 and miR-330-3p (Fig. 2D, E). Circ_0072088 knockdown increased miR-330-3p expression in AML12 cells (Fig. 2F). Together, these observations support a regulatory interaction between circ_0072088 and miR-330-3p.

MiR-330-3p targets the CDK1 3′-UTR

TargetScan analysis identified a potential miR-330-3p-binding site within the CDK1 3′-UTR (Fig. 3A). MiR-330-3p mimics reduced the luciferase activity of the WT CDK1 reporter but did not affect the MUT reporter (Fig. 3B). CDK1 protein levels increased over time following TGF-β1 treatment of AML12 cells (Fig. 3C). MiR-330-3p overexpression reduced CDK1 protein levels (Fig. 3D), whereas miR-330-3p inhibition using AMO-330-3p increased CDK1 protein levels (Fig. 3E). These results support CDK1 as a target of miR-330-3p.

Rescue experiments support the involvement of the miR-330-3p/CDK1 axis

To examine whether miR-330-3p mediates the effects of circ_0072088, AML12 cells were transfected with the circ_0072088 overexpression construct, miR-330-3p mimics, or the corresponding controls, as indicated. Circ_0072088 overexpression reduced E-cadherin levels and increased α-SMA and vimentin levels. Co-transfection with miR-330-3p mimics attenuated these effects (Fig. 4A–D). MiR-330-3p overexpression also reduced the increases in collagen I and IV levels induced by circ_0072088 overexpression (Fig. 4E–G). In addition, miR-330-3p mimics reversed the decrease in cell viability associated with circ_0072088 overexpression (Fig. 4H). These results suggest that miR-330-3p mediates, at least in part, the effects of circ_0072088 on EMT-associated and fibrogenic changes in AML12 cells.

We next investigated whether CDK1 mediates the effects of miR-330-3p. MiR-330-3p overexpression increased E-cadherin levels and decreased α-SMA and vimentin levels, whereas CDK1 overexpression attenuated these changes (Fig. 5A–D). Similarly, CDK1 overexpression reversed the reductions in collagen I and IV levels induced by miR-330-3p overexpression (Fig. 5E–G). These findings support the involvement of CDK1 in the effects of miR-330-3p on EMT-associated and fibrogenic markers.

Finally, we examined whether circ_0072088 regulates CDK1 expression through miR-330-3p. Circ_0072088 knockdown reduced CDK1 protein levels, and

co-transfection with AMO-330-3p reversed this reduction (Fig. 5H). These results are consistent with circ_0072088 regulating CDK1 expression through miR-330-3p.

Discussion

This study identified a potential role for the circ_0072088/miR-330-3p/CDK1 axis in TGF-β1-induced cellular responses in AML12 hepatocytes. Circ_0072088 knockdown increased E-cadherin levels and reduced mesenchymal and ECM-associated protein levels. Interaction assays and rescue experiments supported the involvement of miR-330-3p and CDK1. These findings extend the investigation of circ_0072088 from HCC-related phenotypes to EMT-associated and fibrogenic responses in a hepatocyte model.

EMT-associated processes have been investigated in organ fibrosis [5] and cancer progression [19–21]. TGF-β1-induced changes have also been characterized in hepatic stellate cells, including LX-2 cells[22].In the present study, we examined epithelial, mesenchymal, and fibrogenic markers in AML12 hepatocytes. Circ_0072088 knockdown increased E-cadherin and reduced α-SMA, vimentin, and collagen I and IV levels. These findings indicate a change in the cellular response to TGF-β1; however, marker expression in cultured hepatocytes does not establish that these cells become ECM-producing myofibroblasts in vivo.

CircRNAs are characterized by covalently closed structures, and many exhibit greater stability than linear RNAs[23, 24]. Their functions vary across biological contexts. Circ_0089762 has been implicated in endothelial dysfunction associated with acute myocardial infarction[25],whereas circUBE2I has been linked to lung adenocarcinoma progression through the miR-659-3p/PSMA1 axis[26].Here, bioinformatic prediction and luciferase reporter assays supported an interaction between circ_0072088 and miR-330-3p. Circ_0072088 knockdown increased miR-330-3p expression, and miR-330-3p overexpression attenuated the effects of circ_0072088 overexpression. These observations are consistent with circ_0072088

modulating miR-330-3p-dependent regulation in AML12 cells, although further characterization is needed to establish the endogenous interaction in detail.

MiRNAs regulate gene expression through sequence-dependent interactions with target mRNAs[27]. Several miRNAs have been implicated in liver fibrosis, including miR-26b and miR-149-5p[28, 29], In the present study, miR-330-3p expression decreased following TGF-β1 treatment. MiR-330-3p overexpression attenuated the effects of circ_0072088 overexpression on EMT-associated markers, collagen expression, and cell viability. These findings support a role for miR-330-3p in the cellular responses examined here, while its contribution to liver fibrosis in vivo remains to be established.

CDK1 has been implicated in cancer-related signaling[30]. TargetScan analysis identified a potential miR-330-3p-binding site within the CDK1 3′-UTR, and reporter assays supported this interaction. In AML12 cells, CDK1 protein levels increased following TGF-β1 treatment and were reduced by miR-330-3p overexpression. CDK1 overexpression counteracted the effects of miR-330-3p on EMT-associated and fibrogenic markers. Furthermore, miR-330-3p inhibition reversed the reduction in CDK1 protein levels induced by circ_0072088 knockdown. Together, these findings support the proposed circ_0072088/miR-330-3p/CDK1 regulatory axis.

This study has several limitations. The experiments were conducted in a single hepatocyte cell line, and the proposed mechanism was not evaluated in animal models or clinical samples. The downstream processes linking CDK1 to the observed changes also remain unresolved. Consequently, these results should be interpreted as evidence from an in vitro model. Further studies are needed to establish whether this pathway contributes to liver fibrosis in vivo and whether it can be targeted therapeutically.

Conclusion

Circ_0072088 knockdown attenuated EMT-associated and fibrogenic changes in TGF-β1-treated AML12 hepatocytes. Interaction assays and rescue experiments supported the involvement of the miR-330-3p/CDK1 axis. These findings provide a

basis for further investigation of this regulatory pathway in liver fibrosis, but its relevance in vivo and therapeutic potential require additional validation.

Acknowledgement

Not applicable.

Author Contributions

GL, YC participated in study design. YC, HX, BL, JQ performed the experiments. BL. YC, HX analyzed the data. GL, YC and HX contributed to the writing of the manuscript. All authors read and approved the final version of the manuscript.

Funding

This work was supported by industry-sponsored research project (No.20230517125953).

Availability of data and materials

All data generated or analyzed during this study are included in this published article.

Declarations

Conflict of interest

The authors have no conficts of interest to declare that are relevant to the content of this article.

Ethical approval

This work does not involve animals or human subjects.

Consent for publication

Not applicable.

References

1. Charoenthanakitkul D, Ariyachet C (2026) Decoding fibroblast activation: Transcriptional networks in hepatic stellate cells and across fibrotic organs (Review). Int J Mol Med 58:1–25. https://doi.org/10.3892/ijmm.2026.5962
2. Yang X, Li H, Ye H, et al (2026) Contribution of p38 MAPK in liver fibrosis: An overview of mechanisms, signaling pathways, and therapeutic targets (Review). Int J Mol Med 58:1–32. https://doi.org/10.3892/ijmm.2026.5949
3. Roy D, Hussain MS, Khan Y, et al (2026) AI in the Prediction of Hepatic Fibrosis Progression Using Non-Coding RNAs. Clinica Chimica Acta 587:120973. https://doi.org/10.1016/j.cca.2026.120973
4. Zhong X-H, Li Y, Song Y-K, et al (2026) Breviscapine alleviates liver fibrosis by inhibiting epithelial-mesenchymal transition via TGF-beta1/Smad3 pathway. Journal of Asian Natural Products Research 1–24. https://doi.org/10.1080/10286020.2026.2697867
5. Yu J, Hong X, Zhu T, et al (2026) Visceral adipose stem cell–derived small extracellular vesicles inhibit EMT in renal tubular epithelial cells and attenuate diabetic kidney fibrosis. Biochemical Pharmacology 254:118395. https://doi.org/10.1016/j.bcp.2026.118395
6. Ji X, Chen K, Liu S, et al (2027) Cordyceps militaris granules reduce EMT/ECM marker expression and alleviate pulmonary fibrosis. Journal of Ethnopharmacology 373:122295. https://doi.org/10.1016/j.jep.2026.122295
7. Seo JH, Lee H, Sim DY, et al (2023) Honokiol inhibits epithelial–mesenchymal transition and hepatic fibrosis via activation of Ecadherin/ GSK3B / JNK and inhibition of AKT / ERK /p38/β-catenin/ TMPRSS4 signaling axis. Phytotherapy Research 37:4092–4101. https://doi.org/10.1002/ptr.7871
8. Zhang X, Zhang X, Ge X, Liu M (2022) Mangiferin prevents hepatocyte epithelial-mesenchymal transition in liver fibrosis via targeting HSP27 -mediated JAK2 / STAT3 and TGF -β1/Smad pathway. Phytotherapy Research 36:4167–4182. https://doi.org/10.1002/ptr.7549
9. Liang D, Zheng J, Gao Z, et al (2026) Long non-coding RNAs as master regulators of cancer metastasis and therapeutic resistance. Biochimica et Biophysica Acta (BBA) - Reviews on Cancer 189698. https://doi.org/10.1016/j.bbcan.2026.189698
10. BehnamRassouli R, Entezari F, Ghorbanzadeh M, et al (2026) Non-coding RNAs related to PD1/PD-L1 signaling with potential diagnostic prognostic and therapeutic value in the tumorigenesis of brain cancers. Iranian Journal of Basic Medical Sciences 29:. https://doi.org/10.22038/ijbms.2026.94213.20304
11. Wen Y, Jiang J, Dong W, et al (2026) The cardiac protective human circular RNA circKLHL20_009 sponges miR-31-5p to ameliorate myocardial hypertrophy and fibrosis through suppressing β-catenin signaling. Acta Pharmacol Sin. https://doi.org/10.1038/s41401-026-01912-8
12. Yang G, Zhang S, Cao Y, et al (2026) Circular RNA CIRCLAMC1 Promotes Liver Regeneration by Regulating the MIR -138-5p/Gnai2 Axis. The FASEB Journal 40:e72216. https://doi.org/10.1096/fj.202504443R
13. Ding R, Su D, Zhao Q, et al (2023-3-29) The role of microRNAs in depression. Front Pharmacol 14:1129186. https://doi.org/10.3389/fphar.2023.1129186
14. Li W, Nie A, Jin L, et al (2020) circBIRC6 regulates cisplatin resistance of choroidal melanoma via positively modulating ERK by sponging miR-503-3p

15. Wang S, Qu Y, Liu W, et al (2026) CircRNA0857 acts as an miRNA sponge to promote Newcastle disease virus replication via modulating autophagy. J Virol e01121-26. https://doi.org/10.1128/jvi.01121-26
16. Kumar P, Rawat P, Helal M, et al (2026) Decoding circRNA–miRNA crosstalk in the pathogenesis of hepatic fibrosis: A comprehensive review. International Journal of Biological Macromolecules 371:153022. https://doi.org/10.1016/j.ijbiomac.2026.153022
17. Zhou X, Liang Z, Qin S, et al (2022) Serum-derived miR-574-5p-containing exosomes contribute to liver fibrosis by activating hepatic stellate cells. Mol Biol Rep 49:1945–1954. https://doi.org/10.1007/s11033-021-07008-2
18. Li L, Xiao C, He K, Xiang G (2021) Circ_0072088 promotes progression of hepatocellular carcinoma by activating JAK2 / STAT3 signaling pathway via MIR -375. IUBMB Life 73:1153–1165. https://doi.org/10.1002/iub.2520
19. Ren S, Zhang Y, Hao R, et al (2026) Novel VHL ligand-based PROTACs targeting JNK1: design, synthesis, and biological evaluation with potent anti-EMT activity. Bioorganic Chemistry 181:110388. https://doi.org/10.1016/j.bioorg.2026.110388
20. Yuan S, Li S, Chen C (2026) Hedyotis diffusa Willd-Scutellaria barbata D.Don Suppresses Colorectal Cancer Liver Metastasis by Targeting hsa_circ_0039933-Mediated Epithelial-Mesenchymal Transition. Biochem Genet. https://doi.org/10.1007/s10528-026-11392-4
21. Wang J, Tang J, Wang Y (2026) MXRA5 promotes the progression and metastasis of breast cancer *via* activation of the epithelial-to-mesenchymal transition pathway. Korean J Physiol Pharmacol 30:487–500. https://doi.org/10.4196/kjpp.25.435
22. Carson JP, Robinson MW, Ramm GA, Gobert GN (2021) RNA sequencing of LX-2 cells treated with TGF-β1 identifies genes associated with hepatic stellate cell activation. Mol Biol Rep 48:7677–7688. https://doi.org/10.1007/s11033-021-06774-3
23. Avesani S, Cascione L, Giugno R (2026) Construction and Analysis of circRNA–miRNA–mRNA Regulatory Networks. In: Laganà A, Nigita G (eds) MicroRNA Target Identification. Springer US, New York, NY, pp 197–214
24. Galli V, Vinciguerra S, Biagioli M, Morandell J (2025-5-16) Circular RNAs as disease modifiers of complex neurologic disorders. Front Pharmacol 16:1577496. https://doi.org/10.3389/fphar.2025.1577496
25. Zhao Y, Lu P, Lu X, Liu Z (2026) Circulating Circ_0089762 Predicts Adverse Outcomes in Acute Myocardial Infarction Via Regulating miR-938/STAT3-Mediated Endothelial Dysfunction. Cardiovasc Drugs Ther. https://doi.org/10.1007/s10557-026-07910-6
26. Xue P, Gao Y, Li T, et al (2026) CircUBE2I regulates YAP/TAZ signaling pathway through miR-659-3p/PSMA1 axis to promote human lung adenocarcinoma cell progression. Experimental Cell Research 462:115157. https://doi.org/10.1016/j.yexcr.2026.115157
27. Sharma G, Lamichhane S, Chae S-C (2026) MIR133A in Cancer Biology: Target Genes, Biological Effects, and Biomarker Potential. Genes 17:781. https://doi.org/10.3390/genes17070781
28. Xu J, He L, Xu J, et al (2026) miR-26b-modified human umbilical cord mesenchymal stem cells exhibit enhanced anti-fibrotic efficacy in a mouse model of hepatic fibrosis. Mol Biol Rep 53:1376. https://doi.org/10.1007/s11033-026-12414-5
29. Zhou J-C, Xu A-J, Miao J, et al (2026) miR149-5p: A hepatocyte EXOmotif sequence

containing microRNA that attenuates liver fibrosis by specifically targeting PDGFRB in HSCs. Journal of Advanced Research S2090123226006302. https://doi.org/10.1016/j.jare.2026.08.021

30. Lai Y, Liu R, Zhou L, et al (2026) The astragaloside-brucea javanica oil nanoemulsion inhibiting the progression of oral squamous cell carcinoma through CDK1-HOXC10-MTFR2 pathway. Bioorganic Chemistry 178:109983. https://doi.org/10.1016/j.bioorg.2026.109983

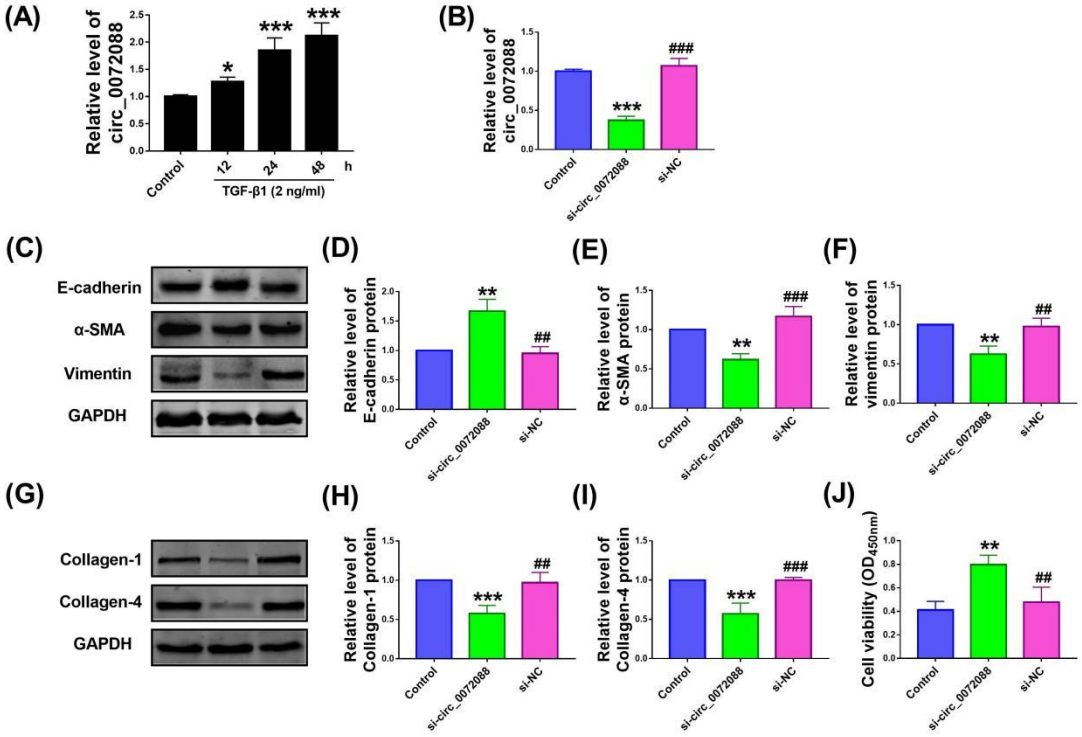

Fig. 1 Circ_0072088 knockdown attenuates EMT-associated and fibrogenic changes in AML12 cells. (A) Circ_0072088 expression following TGF-β1 treatment. (B) Circ_0072088 expression after transfection with si-circ_0072088 or si-NC. (C) Representative western blots of E-cadherin, α-SMA, and vimentin. (D–F) Densitometric quantification of the proteins shown in C. (G) Representative western blots of collagen I and IV. (H, I) Densitometric quantification of collagen I and IV. (J) Cell viability assessed using the CCK-8 assay. *P < 0.05, **P < 0.01, ***P < 0.001 versus control; ##P < 0.01, ###P < 0.001 versus si-circ_0072088. n = 5. All blots were cropped from different gels.

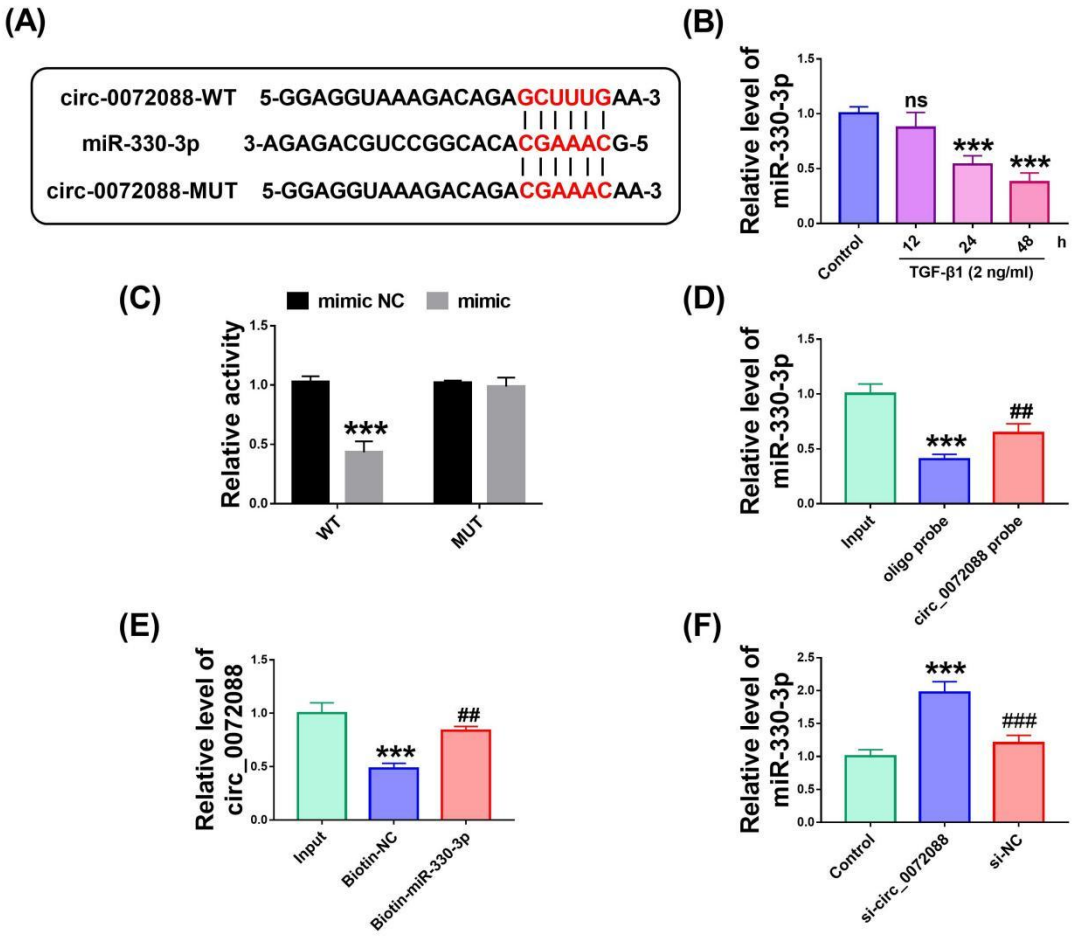

Fig. 2. Interaction between circ_0072088 and miR-330-3p. (A) Predicted miR-330-3p-binding site in circ_0072088 and the corresponding mutant sequence. (B) MiR-330-3p expression in TGF-β1-treated AML12 cells. (C) Luciferase reporter analysis of the WT and MUT circ_0072088 constructs. ***P < 0.001 versus mimic NC. (D, E) RNA interaction assays examining circ_0072088 and miR-330-3p in AML12 cells. ***P < 0.001 versus input; ##P < 0.01 versus NC. (F) MiR-330-3p expression following circ_0072088 knockdown. ***P < 0.001 versus control; ###P < 0.001 versus si-circ_0072088. n = 5.

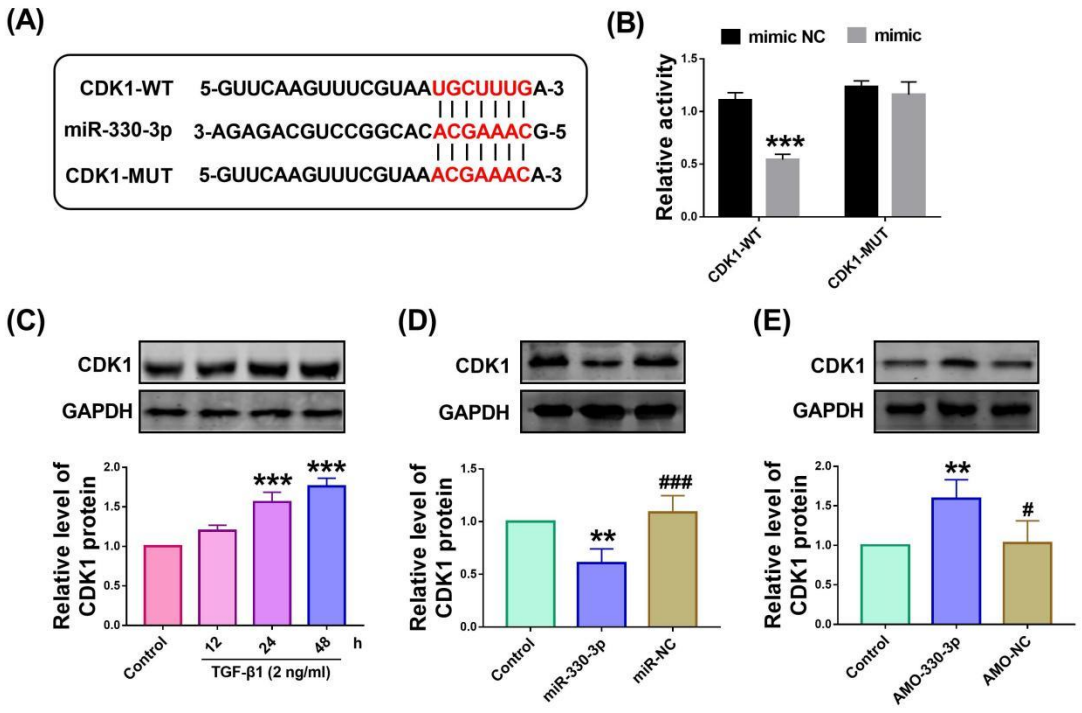

Fig. 3 MiR-330-3p targets the CDK1 3′-UTR. (A) Predicted miR-330-3p-binding site within the CDK1 3′-UTR and the corresponding mutant sequence. (B) Luciferase activities of the WT and MUT CDK1 reporter constructs in HEK293T cells. (C) CDK1 protein levels in TGF-β1-treated AML12 cells. ***P < 0.001 versus control. (D) CDK1 protein levels following miR-330-3p overexpression. **P < 0.01 versus control; ###P < 0.001 versus miR-330-3p. (E) CDK1 protein levels following miR-330-3p inhibition using AMO-330-3p. #P < 0.05 versus AMO-330-3p. n = 5. All blots were cropped from different gels.

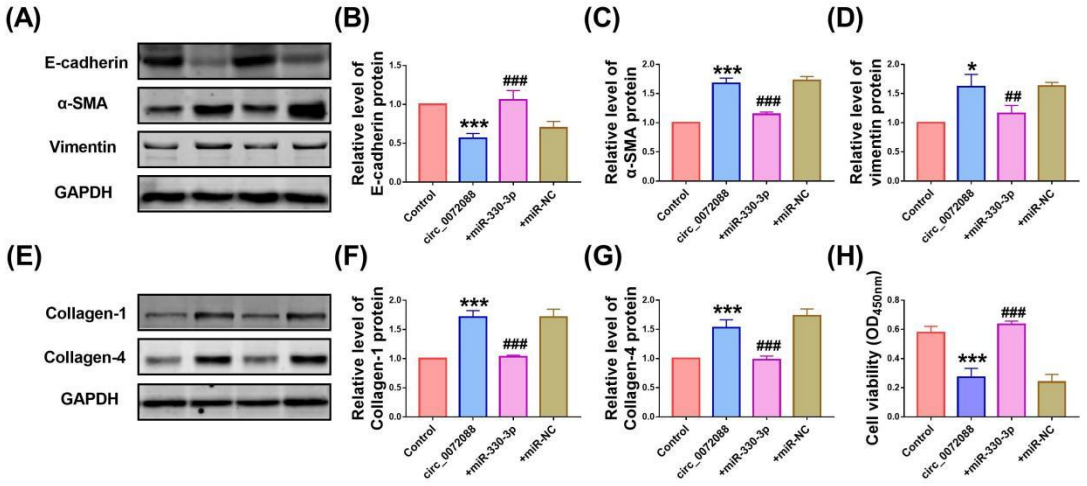

Fig. 4 MiR-330-3p overexpression attenuates the effects of circ_0072088 overexpression. (A) Representative western blots of E-cadherin, α-SMA, and vimentin. (B–D) Densitometric quantification of the proteins shown in A. *P < 0.05, ***P < 0.001 versus control; ##P < 0.01, ###P < 0.001 versus circ_0072088. (E) Representative western blots of collagen I and IV. (F, G) Densitometric quantification of collagen I and IV. ***P < 0.001 versus control; ###P < 0.001 versus circ_0072088. (H) Cell viability assessed using the CCK-8 assay. ***P < 0.001 versus control; ###P < 0.001 versus circ_0072088. n = 5. All blots were cropped from different gels.

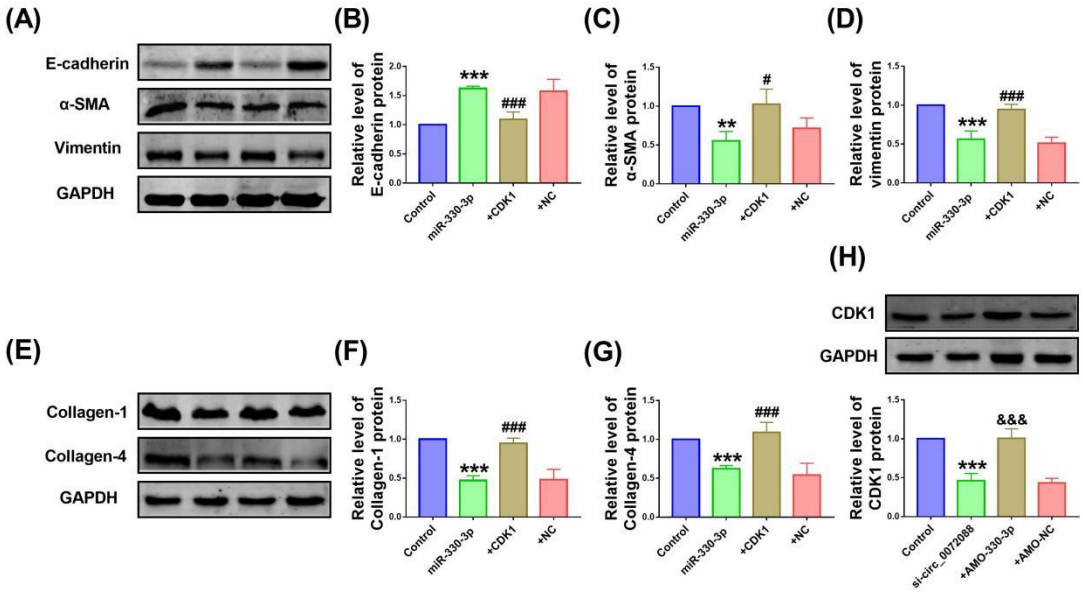

Fig. 5 CDK1 overexpression counteracts the effects of miR-330-3p, and miR-330-3p inhibition reverses the effect of circ_0072088 knockdown on CDK1. (A) Representative western blots of E-cadherin, α-SMA, and vimentin. (B–D) Densitometric quantification of the proteins shown in A. **P < 0.01, ***P < 0.001 versus control; #P < 0.05, ###P < 0.001 versus miR-330-3p. (E) Representative western blots of collagen I and IV. (F, G) Densitometric quantification of collagen I and IV. ***P < 0.001 versus control; ###P < 0.001 versus miR-330-3p. (H) CDK1 protein levels following transfection with si-circ_0072088, AMO-330-3p, or AMO-NC, as indicated. ***P < 0.001 versus control; &&&P < 0.001 versus si-circ_0072088. n = 5. All blots were cropped from different gels.